Tight blood glycaemic and blood pressure control in experimental diabetic nephropathy reduces extracellular matrix production without regression of fibrosis

Tight blood glycaemic and blood pressure control in experimental diabetic nephropathy reduces extracellular matrix production without regression of fibrosis

[1]Bryan R. Conway, [2]Boris Betz, [2]Tara A. Sheldrake, [1]Jonathan R. Manning, [1]Donald R. Dunbar, [3]Abigail Dobyns, [2,4]Jeremy Hughes, [1,4]John J. Mullins

[1]British Heart Foundation/University of Edinburgh Centre for Cardiovascular Science

[2]Centre for Inflammation Research, University of Edinburgh, UK

[3]Department of Bioengineering, University of Illinois at Chicago, USA

[4]These authors contributed equally to this work

Running head: Glycaemic/blood pressure control in experimental DN

Corresponding author

Dr Bryan Conway,

Room W3.06,

BHF/UoE Centre for Cardiovascular Science,

Queen's Medical Research Institute,

47 Little France Crescent,

Edinburgh

EH16 4TJ

Tel: +44 (0)131 2426691 FAX: +44 (0)131 2426779

This article has been accepted for publication and undergone full peer review but has not been through the copyediting, typesetting, pagination and proofreading process, which may lead to differences between this version and the Version of Record. Please cite this article as doi: 10.1111/nep.12335

Word count: Abstract: 247 Body: 4248

Abstract

Aims Regression of albuminuria and renal fibrosis occurs in patients with diabetic nephropathy (DN) following tight control of blood glucose and blood pressure, however the pathways that promote regression remain poorly understood and we wished to characterise these using a rodent model.

Methods Diabetes was induced with streptozotocin in Cyp1a1mRen2 rats and hypertension was generated by inducing renin transgene expression with dietary indole-3-carbinol (I-3-C) for 28wks. At this point an 'injury cohort' was culled, while in a 'reversal cohort' glycaemia was tightly controlled using insulin implants and blood pressure normalised by withdrawing dietary I-3-C for a further 8wks. Pathways activated during and following reversal of diabetes and hypertension were assessed by microarray profiling.

Results Tight control of blood glucose and blood pressure reduced albuminuria and renal hypertrophy, but had no impact on renal fibrosis. 85 genes were up-regulated specifically during the injury phase, including genes encoding multiple myofibroblast and extracellular matrix (ECM) proteins. Conversely, 314 genes remained persistently elevated during reversal including genes linked to innate/adaptive immunity, phagocytosis, lysosomal processing and degradative metalloproteinases (MMPs). Despite increased MMP gene expression, MMP activity was suppressed during both injury and reversal, in association with up-regulation of tissue inhibitor of metalloproteinase-1 (TIMP-1) protein. Physical separation of the TIMP-1/MMP complexes during zymography of tissue homogenate restored MMP activity.

Conclusion Normalisation of blood glucose and pressure ameliorates albuminuria and inhibits excess ECM production, however persistent TIMP-1 expression hinders attempts at ECM remodelling. Therapies which counteract the action of TIMPs may accelerate scar resolution.

Keywords: diabetic nephropathy, fibrosis, hyperglycaemia, hypertension, fibrosis, regression

Introduction

As with many chronic diseases, the rate of progression of diabetic nephropathy (DN) depends on the net balance between the severity of the injury and the body's reparative capacity, such that a reduction in injurious stimuli may facilitate regression of disease. There is precedent for this in diabetic kidney disease as tight control of the pre-eminent factors promoting injury, namely hyperglycaemia and hypertension, can result in regression of microalbuminuria[1]. Furthermore, a reduction in glomerulosclerosis[2] and tubulointerstitial fibrosis[3] has been documented in patients with moderately advanced DN who achieved sustained normoglycaemia following pancreas transplantation. Resolution of fibrosis is, however, a protracted process, requiring up to 10 years of normoglycaemia.

While considerable research has focused on the pathways that promote disease, less is known about mechanisms of repair. This is partly due to the scarcity of kidney tissue available from patients during regression of DN, as there is little rationale for performing renal biopsy in this setting. Furthermore, the regression has been difficult to study in an experimental setting as traditional animal models exhibit only the earliest features of human disease[4].

We recently described a rodent model in which hyperglycaemic and renin-dependent hypertension synergise to promote transcriptomic and pathological changes typical of moderately advanced human DN[5]. An attractive feature of this model is that the Cyp1a1mRen2 rats have a copy of the murine *ren2* cDNA integrated into their genome under the control of the Cyp1a1 promoter, such that the severity of hypertension can be regulated by altering the dietary concentration of indole-3-carbinol (I-3-C)[6].

The aim of the current study was to identify pathways that were differentially regulated in the kidney during and following reversal of hyperglycaemia and hypertension in the Cyp1a1mRen2 model using systematic gene expression profiling.

Materials and methods

Animal studies

Diabetes was induced in adult, male Cyp1a1mRen2 Fisher rats with an intravenous bolus of 20mg/kg streptozotocin and confirmed by blood glucose >15mM three days later. Thereafter, blood glucose was maintained between 20-30mM with serial subcutaneous insulin implants (Research Pack, Linshin, Canada). Two weeks after streptozotocin, 0.125% I-3-C (Sigma, UK) was added to the diet to maintain tail-cuff systolic BP at approximately 200mmHg. At the end of the 28wk 'injury phase' the animals were randomised into two groups matched for blood glucose, blood pressure and albuminuria. An injury cohort (n=10) was culled immediately, while in a reversal cohort (n=9) the blood glucose concentration was tightly controlled by increasing the frequency/dose of the insulin implants and I-3-C was removed from the diet to facilitate normalisation of blood pressure for a further eight weeks (Fig 1A). Six age-matched, male, non-diabetic, non-hypertensive controls were culled at 28wks. Procedures were performed under UK Home Office licence following approval by the Ethics Committee, University of Edinburgh.

Quantification of proteinuria and renal function

24hr urine collections were obtained at baseline, 9, 18 and 28wks and at 1, 2, 4, 6 and 8wks after reversal. Tail vein blood samples were taken at baseline, after 28 weeks of injury and eight weeks of reversal. Albumin and creatinine measurements were performed on a Cobas Fara centrifugal analyser (Roche Diagnostics Ltd, UK) using a commercial immunoturbidimetric assay (Microalbumin Kit, Olympus Diagnostics Ltd, Watford, UK) and a creatininase-based enzymatic method (Alpha Laboratories Ltd, Eastleigh, UK), respectively.

Immunohistochemistry

Immunohistochemistry was performed using standard protocols on 4μM methacarn-fixed sections (for transgelin, ED-1, CD3, WT1) or paraformaldehyde-fixed, paraffin-embedded sections following antigen retrieval with 10mM Tris Base/1mM EDTA (for inducible nitric oxide synthase (iNOS) and mannose receptor). Primary antibodies included: rabbit anti-mouse transgelin (1:8,000, Abcam, Cambridge, UK), mouse anti-rat ED-1 (1:100, AbD Serotec, Kidlington, UK), rabbit anti-rat iNOS (1:2,500, Abcam, Cambridge, UK), rabbit anti-rat Mannose Receptor (1:1,500, Abcam, Cambridge, UK), rabbit anti-human CD3 (1:100, DAKO, Cambridge, UK) and rabbit anti-human WT1 (1:200, Santa Cruz Biotechnology, Santa Cruz, CA, USA) followed by a species-appropriate, biotinylated secondary antibody (1:300, Vector Labs, Peterborough, UK) and detection with the Vector ABC kit and DAB. Sections were also stained for periodic acid-schiff and picrosirius red with glomerulosclerosis and tubulointerstitial fibrosis indices determined from a mean of 150 glomeruli and 25 x200-power tubulointerstitial fields per animal, respectively. For both indices a semi-quantitative scoring system was devised: grade 0: normal; grade 1: <25%; grade 2: 25-50%; grade 3: 50-75% and grade 4: >75% of area sclerosed/fibrosed. Glomerulosclerosis/TIF indices = $(1 \times n_1) + (2 \times n_2) + (3 \times n_3) + (4 \times n_4)$/total number of glomeruli/tubulointerstitial fields scored, where n_1-n_4 are the number of fields in each of grades 1-4. The mean number of infiltrating ED-1^+, iNOS$^+$ and MR$^+$ macrophages and CD3$^+$ T-cells were obtained from 20-30 x400 tubulointerstitial fields/animal. The mean number of glomeruli was calculated after counting the total number of glomeruli per kidney section in each animal. The mean glomerular surface area was obtained by manually tracing the glomerular tuft of all hilar glomeruli present in a kidney section from each animal (20-30 glomeruli per section) using an image analysis system (Adobe Photoshop Software). The mean number of WT1+ cells was calculated by counting the number of WT1$^+$ nuclei in 20-30 hilar glomerular cross-sections/animal.

Gene expression analysis

RNA was extracted (Nucleospin RNAII kit, Macherey-Nagel, Duren, Germany) from snap-frozen, homogenised renal cortices from representative animals from the injury cohort (n=8), the reversal cohort (n=4) and from controls (n=4) and hybridized to the Affymetrix Rat Genome 230 2.0 GeneChip. Data were extracted by GCOS software, and CEL files were further processed in Bioconductor, normalized by RMA in the Affy module, and analysed with the Limma package. Data are available in the ArrayExpress database (accession no:E-MEXP-3739). Pathway enrichment analysis was performed using the Gene Ontology/KEGG tools on DAVID, Metacore (GeneGo, St. Joseph, MI, USA) or Ingenuity (Qiagen, Redwood City, CA, USA). The relative expression of selected genes was validated in all animals by rtPCR using the 2-ΔΔCt method and Taqman assays (Applied Biosystems, Cheshire, UK): *tagln*:Rn01642285_g1; *acta2*:Rn01759928_g1; *col1a1*:Rn01463848_m1; *fn*:Rn00569575_m1; *foxp3*:Rn01525092_m1; *mmp2*:Rn01538170_m1; *mmp7*:Rn00689241_m1; *mmp12*:Rn00588640_m1; *mmp14*:RN00579172_m1; *timp1*:Rn01430873_g1; *timp2*:Rn00573232_m1; *timp3*:Rn00441826_m1.

Metalloproteinase activity assay/zymography

For the MMP activity assay/zymography, frozen renal cortex was homogenised (20%v/w) in RIPA lysis buffer or 150mM NaCl/1% Triton X-100/50mM Tris, respectively, and normalised for protein concentration (BCA assay, Thermo Scientific, Northumberland, UK). Metalloproteinase activity was assessed using the EnzChek™ Gelatinase/Collagenase Assay Kit (Invitrogen) employing the gelatinase/collagenase inhibitor 1,10-phenanthroline, monohydrate as a negative control.

For substrate zymography polyacrylamide gels were co-polymerized with either gelatin (1mg/ml) or collagen (0.2mg/ml) and 100µg lysate per lane was separated by electrophoresis. Gels were washed twice with 2.5% Triton X-100, incubated at 37°C for 48-72 hours (Bio-Rad, Hercules, CA), stained with 0.05% Coomassie Brilliant Blue (VWR, Radnor, USA) in

methanol/acetic acid/water and de-stained in aqueous 4% methanol/8% acetic acid. Band intensities were quantified on Software Odyssey v.3.0 (Li-Cor, Lincoln, USA).

Western blotting

Renal cortices were homogenised in 150 mM NaCl/20 mM Tris-HCl/1mM EDTA (pH8)/1% Triton-X 100/protease inhibitor cocktail (Roche, Switzerland). 30 μg protein was separated on a 10% SDS gel, transferred to a membrane and incubated with rabbit anti-rat TIMP-1 antibody (1: 1000, Biorbyt, Cambridge, UK) or rabbit anti-rat β-actin (1 : 1000, Abcam, Cambridge, UK) and horseradish peroxidase-conjugated anti-rabbit IgG secondary (1 : 2,000, Dako, Hamburg, Germany). Recombinant TIMP1 (RayBiotech, Norcross, USA) constituted a positive control. Blots were developed using a chemiluminescence kit (ECL Plus, Amersham, GE Healthcare, Buckinghamshire, UK), imaged on a Versadoc system (Bio-Rad, Hercules, USA) and densitometry was performed using Adobe Photoshop Software.

Statistical analysis

Data are means (±SEM) and medians (IQR) where normal or skewed, respectively. Groups were compared by 1-way ANOVA followed by Bonferroni corrections (following log-transformation of non-parametric data). The Benjamini-Hochberg false-discovery rate method was used to correct for multiple testing in microarray analysis.

Results

Biochemical parameters

During the 28wk injury phase, there was a progressive rise in albuminuria (Fig 1B-D). In the reversal cohort, an increase in the dose and frequency of subcutaneous insulin implants ameliorated hyperglycaemia (Fig 1B) while removal of 1-3-C from the diet normalised systolic blood pressure (Fig 1C). This led to a rapid initial reduction in albuminuria probably related to haemodynamic factors followed by a more gradual decline, though it remained

persistently greater than in controls (Fig 1D). After 28wks of diabetes and hypertension, creatinine clearance was not significantly different in either the injury (2.45±0.87ml/min) or reversal cohorts (2.46±0.30ml/min) compared with controls (2.37±0.63ml/min, p=0.48 and p=0.64, respectively) and remained unchanged following 8wks of relative normalisation of glycaemia and blood pressure (2.59±0.63ml/min, p=0.56 v peak injury).

Pathological parameters

The mean percentage kidney:body weight ratio increased in the injury cohort compared with controls (0.47±0.06 v 0.30±0.01, p<0.001, Table 1). This reduced in the reversal cohort (0.36±0.03, p<0.001 v injury cohort) though it remained significantly (p<0.05) greater than in controls. There was a marked increase in the glomerulosclerosis and tubulointerstitial fibrosis indices in the injury cohort compared with controls (Fig 2). After 8wks of tight blood glucose and blood pressure control, the reversal cohort exhibited similar severity of glomerulosclerosis and tubulointerstitial fibrosis to the injury cohort, and significantly greater levels than controls (Fig 2). There were no differences between the groups in the mean hilar glomerular cross-sectional area or mean number of glomeruli per tissue section (Table 1). While there was a trend towards a reduction in the mean number of $WT1^+$ podocytes/hilar glomerular cross-sectional in the injury and reversal cohorts compared with control animals, this did not reach statistical significance (p=0.07, Suppl Figure).

Microarray data

To identify pathways activated in the kidney during and following reversal of hyperglycaemia and hypertension, we compared gene expression patterns in the renal cortices of the injury and reversal cohorts with controls. 677 genes were up-regulated >1.5-fold (corrected p<0.01) in the injury cohort compared with controls. The expression of 85 of these fell >50% towards control levels following 8wks of reversal of hyperglycaemia and hypertension ('Up-regulated specifically during injury', Fig 3, Suppl Table 1). Conversely the expression of 314 genes remained persistently increased (increased further or fell <20%

compared to peak injury) despite 8wks of relative normoglycaemia and normotension ('Persistently up-regulated', Fig 3, Suppl Table 2).

145 genes were down-regulated >50% in the injury cohort compared with controls (corrected $p<0.01$). The expression of 80 of these 145 genes did not increase significantly (<20% increase compared to peak injury) after 8wks of reversal of hyperglycaemia and hypertension and were designated as 'persistently repressed' (Figure 3 and Suppl Table 3). Conversely, there was a significant (corrected $p<0.05$) increase in the expression of 4 of the 145 down-regulated genes (Von Willebrand factor, phospholipase A2 group 6, malic enzyme 1, and lactate dehydrogenase D), such that they were no longer differentially expressed compared to controls (designated 'de-repressed' Fig 3).

Finally, the expression of a small number of genes did not change during injury but was significantly (corrected $p<0.05$) down-regulated (n=19) or up-regulated (n=5) after 8wks of reversal of hyperglycaemia or hypertension (Fig 3, Suppl Table 4). Remarkably, 12/19 genes (63%) that were down-regulated specifically during reversal encoded for proteins selectively expressed on endothelial cells.

Validation of microarray findings

Pathway analysis using both Ingenuity and Metacore (Table 2) determined that many of the genes that were up-regulated specifically during injury are implicated in acute phase response, complement/coagulation pathways and regulation of the ECM. The pattern of expression of selected ECM-related genes was validated by real-time PCR (Fig 4A).

Amongst the genes whose expression remained persistently up-regulated during reversal there was an over-representation of genes implicated in innate and adaptive immunity, ECM degradation, Wnt pathway and apoptosis (Table 3). Consistent with the transcriptomic data, increased numbers of macrophages were found in both the injury and reversal cohorts (Fig 4Bi), however there was a switch in macrophage phenotype, with increased classically activated $iNOS^+$ macrophage infiltration occurring exclusively during injury (Fig 4Bii),

whereas infiltrates of mannose receptor $(MR)^+$ macrophages were observed both during and following reversal of injury (Fig 4Biii). T-cells infiltrated the interstitium of both the injury and repair cohorts (Fig 4Ci) and interestingly, there was persistent increase in expression of the *foxp3* gene, a marker of regulatory T-cells (T_{Reg}) (Fig 4Cii).

Metalloproteinase activity assays

Real-time PCR confirmed that the expression of multiple matrix metalloproteinase (MMP) genes was increased during injury, with *mmp-7* and *-12* remaining up-regulated or even increasing during reversal, while *mmp-2,* and *-14* partially reverted towards control levels (Fig 5A). Despite the increase in MMP gene expression, there was a paradoxical decrease in MMP activity in the renal cortex during both injury and reversal as assessed by gelatinase and collagenase activity assays (Fig 5B). Gene expression of tissue inhibitor of metalloproteinase-1 (*timp-1*), and to a lesser extent *timp-2*, increased during injury (Fig 5Ci), and while expression of the *timp-1* gene fell significantly during reversal, TIMP-1 protein remained persistently elevated compared to controls (Fig 5Cii). In contrast to the reduced MMP activity in whole kidney lysates, when TIMPs were physically separated from the MMPs during gel zymography, MMP-2 (72kD band in gelatinase zymogram, Fig 5Di) and MMP-1 (52kD band in collagenase zymogram, Fig 5Dii) activity in both the injury and reversal cohorts tended to be greater than in controls, and indeed MMP-1 activity was significantly greater during reversal than in controls.

Discussion

In our rodent model of moderately advanced DN, relative normalisation of hyperglycaemia and hypertension for eight weeks reduced albuminuria and renal hypertrophy but did not lead to regression of established renal scarring. This is in contrast to previous studies in which scar regression was observed after a similar duration of tight glycaemic control or renin-angiotensin system blockade, however these studies were performed in non-diabetic models[7]

[8 9] or in models of early diabetic injury[10]. The current findings must be considered in the context of human disease, where regression of fibrosis in the diabetic kidney is a protracted process, requiring ten years of normoglycaemia following pancreatic transplantation, with no improvement documented after five years[2].

There is scant data regarding how the diabetic kidney responds to a period of tight blood glucose and blood pressure control. The patterns of gene expression in the kidney of diabetic and hypertensive Cyp1a1mRen2 rats have been shown to closely reflect those in human disease[5], therefore we considered it an appropriate model in which to dissect the pathways activated in the kidney during and following reversal of hyperglycaemia and hypertension. Our study provides insight into the mechanisms that promote fibrosis and a rationale as to why the diabetic kidney is so resistant to repair.

The 85 genes that were up-regulated specifically during the injury phase were markedly enriched for genes encoding ECM proteins, suggesting that tight blood glucose and blood pressure control was sufficient to switch off excess ECM production and prevent progression of fibrosis. Within this group were multiple myofibroblast markers including transgelin, platelet-derived growth factor-β and α-smooth muscle actin, which is consistent with the role of the myofibroblast as the chief scar-producing cell in the kidney[11]. We hypothesise that many of the other genes that are similarly up-regulated specifically during the injury phase (Suppl table 1) may also be implicated in the pro-fibrotic response, and evidence from fibrosis in other organs supports this concept. The lysyl oxidase and lysyl oxidase-like 2 genes are both up-regulated in liver and lung fibrosis, where they mediate collagen cross-linkage, rendering it resistant to degradation.[12] Similarly, the cadherin 11 gene is up-regulated in idiopathic pulmonary fibrosis with administration of a neutralising antibody against CDH11 proving beneficial in experimental lung fibrosis[13]. In addition, pathway analysis of genes up-regulated during the injury phase demonstrated enrichment with acute phase

response and complement genes, which are classically associated with acute renal injury, but have been recently recognised to be activated in human DN[14].

We observed a much larger group of genes that remain up-regulated despite tight blood glucose and blood pressure control. We hypothesise that these may constitute a thwarted attempt at repair, remaining persistently up-regulated in a bid to restore normal tissue homeostasis. Prominent amongst these persistently up-regulated genes are those linked to innate and adaptive immunity. T-cell infiltration has been documented in the kidneys of patients with DN[15], however their role is uncertain as they may promote albuminuria[16], whereas specific subsets, such as T_{reg} cells, may mediate repair[17]. The persistent increase in gene expression of the T_{reg} cell marker, *foxp3*, supports such a reparative role following reversal of diabetes and hypertension. Macrophages also may have both detrimental and beneficial effects, with classically activated macrophages promoting nephropathy[18], while 'reparative' macrophages are essential both for regeneration of injured renal tubules and for resolution of fibrosis[19]. Our data suggests that during hyperglycaemia and hypertension, there is an influx of injurious classically activated $iNOS^+$ macrophages, which become deactivated, emigrate or apoptose during the reversal phase. Conversely, MR^+ 'reparative' macrophages infiltrate the diabetic kidney and persist despite tight blood glucose and blood pressure control. In parallel, there is persistent up-regulation of genes that encode macrophage proteins involved in matrix degradation, phagocytosis and lysosomal processing, a genetic signature that is characteristic of a reparative macrophage phenotype[20]. Furthermore, the Wnt and Ephrin, and Nrf2 signalling pathways were over-represented amongst genes that remained up-regulated despite reversal of diabetes and hypertension, which is of interest, given that all these pathways have been associated with repair in other models of renal injury[21-23]. Taken together, the switch in macrophage polarisation and pathway analysis suggests attempts at repair are initiated, however we cannot exclude the possibility that some of the gene

expression changes are due to residual injury due to modest hyperglycaemia or ongoing albuminuria.

Our study offers insight as to why the reparative pathways that are initiated in the diabetic kidney are relatively ineffectual in degrading excess ECM. Despite a marked increase in MMP gene expression, the MMP activity was reduced to a comparable level to that observed following addition of a biochemical inhibitor of MMP activity. This suggests that an endogenous inhibitor of MMPs may be present, and a likely candidate is TIMP-1 protein, which is persistently expressed in both injury and reversal phases. Furthermore, the non-covalent nature of the TIMP:MMP interaction facilitated physical separation of the TIMPs from MMPs during gel zymography, and under these conditions the activity of both a collagenase, MMP-1, and a gelatinase, MMP-2, increased substantially. TIMP-1 is also up-regulated in human diabetic nephropathy[24] and strategies to block the action of TIMP-1 *in vivo*, thereby facilitating the ECM-degrading activity of the up-regulated MMPs, may be an attractive therapeutic target in DN. While this strategy has proven beneficial in rodent models of cirrhosis[25], the role of MMPs and TIMPs in renal fibrosis is complex as MMPs may also exert detrimental effects by activating multiple pro-inflammatory pathways, therefore the efficacy and safety of TIMP-1 antagonism must be confirmed initially in rodent studies.

In our microarray profiling we identified that the majority of the 145 genes which were down-regulated in the injury cohort continued to be expressed at reduced levels during reversal. While this may reflect an important functional transcriptomic response of surviving nephrons to injury, it is perhaps more likely that it simply reflects a loss of nephron mass as this subset included structural genes, such as nephrin. Consistent with this hypothesis, there was a trend towards a persistent reduction in the number of WT1+ cells/glomerular cross-section, suggesting that tight glycaemic and blood pressure control was insufficient to restore nephron mass, and that additional therapies may be required to promote regeneration of nephrons. Interestingly, more than half of the genes that were specifically down-regulated

during reversal are found relatively selectively on endothelial cells. The significance of this is uncertain and will be the focus of further investigation.

We acknowledge that our study has several limitations. As we reversed both hyperglycaemia and hypertension simultaneously, we cannot determine which of these factors was primarily responsible for the findings observed during reversal. Furthermore, our ability to rapidly switch off the mRen2 transgene, enabled blood pressure to be almost normalised, which is not always achieved in patients with DN. However, we considered that with suboptimal blood pressure control or removal of single injurious stimulus, the presence of on-going injury would preclude identification of pathways that promoted repair. Similarly, the study was not designed to differentiate between the effects of a reduction in blood pressure versus de-activation of the renin-angiotensin system *per se*. While the period of blood glucose and blood pressure control was of similar duration to that employed in other rodent studies[7-10], in this more advanced model of DN it may be that a longer period is required for regression to occur, as in human disease[2]. Finally, an additional cohort of animals that were maintained diabetic and hypertensive throughout the 36 week period would have been helpful in determining whether the reduction in expression of pro-fibrotic genes observed during the reversal phase was sufficient to prevent further progression of DN, however this was not the primary focus of the current study. Furthermore, the reversal cohort at 36wks was compared with the control and injury groups at 28wks, therefore it is possible that the reversal group sustained further renal injury during the additional 8 weeks despite reversal of diabetes and hypertension due to other factors such as aging, brief hyperglycaemic excursions or the effects of anaesthesia during insertion of insulin pellets. This may have biased against observing a reduction in renal fibrosis

In summary, tight control of blood glucose and blood pressure in a novel model of DN is sufficient to ameliorate albuminuria and switch off excess ECM production but does not lead to regression of scarring or restoration of nephron mass. Transcriptomic profiling has

identified genes associated with the fibrotic response, some of which have previously been implicated in fibrosis in the kidney and other organs, while others represent novel anti-fibrotic targets. The data suggest that reparative pathways are initiated, but may be thwarted by the continued presence of TIMPs. Further research is warranted to determine whether strategies that counteract the inhibitory properties of TIMPs may accelerate resolution of fibrosis in the diabetic kidney.

Acknowledgements

We acknowledge the assistance of Dr Forbes Howie in performing the albumin and creatinine assays and the technical support from staff of the University of Edinburgh Animal Facility. B.C. was supported by a MRC Clinician Scientist Fellowship and a Fellowship Transition Award from the British Heart Foundation Centre of Research Excellence (CoRE). J.R.M. and D.D. were supported by the BHF CoRE. B.B. was supported by the European Renal Association-European Dialysis and Transplantation Association Fellowship Programme. The study was part funded by an innovation grant from Kidney Research, UK and the Lothian Renal Endowment Fund.

Contributions

B.R.C, B.B. and T.A.S carried out the animal study and performed the experiments. B.R.C, J.R.M and D.R.D analysed the results. B.R.C, J.H and J.J.M conceived the idea for the study. B.R.C wrote the manuscript which was edited by all the authors. B.R.C will act as guarantor for the article.

Disclosures

The authors declare no conflict of interest with respect to the manuscript.

References

1. Perkins BA, Ficociello LH, Silva KH, Finkelstein DM, Warram JH, Krolewski AS. Regression of microalbuminuria in type 1 diabetes. *N Eng J Med* 2003;348(23):2285-93.

2. Fioretto P, Steffes MW, Sutherland DER, Goetz FC, Mauer M. reversal of lesions of diabetic nephropathy after pancreas transplantations. *N Eng J Med* 1998;339:69-75.

3. Fioretto P, Sutherland DE, Najafian B, Mauer M. Remodeling of renal interstitial and tubular lesions in pancreas transplant recipients. *Kidney Int* 2006;69(5):907-12.

4. Brosius FC, 3rd, Alpers CE, Bottinger EP, et al. Mouse models of diabetic nephropathy. *J Am Soc Nephrol* 2009;20(12):2503-12.

5. Conway BR, Rennie J, Bailey MA, et al. Hyperglycemia and renin-dependent hypertension synergize to model diabetic nephropathy. *J Am Soc Nephrol* 2012;23(3):405-11.

6. Kantachuvesiri S, Fleming S, Peters J, et al. Controlled hypertension, a transgenic toggle switch reveals differential mechanisms underlying vascular disease. *J Biol Chem* 2001;276(39):36727-33.

7. Adamczak M, Gross ML, Krtil J, et al. Reversal of glomerulosclerosis after high-dose enalapril treatment in subtotally nephrectomized rats. *J Am Soc Nephrol* 2003;14(11):2833-42.

8. Remuzzi A, Gagliardini E, Sangalli F, et al. ACE inhibition reduces glomerulosclerosis and regenerates glomerular tissue in a model of progressive renal disease. *Kidney Int* 2006;69(7):1124-30.

9. Hayashi K, Sasamura H, Ishiguro K, Sakamaki Y, Azegami T, Itoh H. Regression of glomerulosclerosis in response to transient treatment with angiotensin II blockers is attenuated by blockade of matrix metalloproteinase-2. *Kidney Int* 2010;78(1):69-78.

10. Pichaiwong W, Hudkins KL, Wietecha T, et al. Reversibility of structural and functional damage in a model of advanced diabetic nephropathy. *J Am Soc Nephrol* 2013;24(7):1088-102.

11. Meran S, Steadman R. Fibroblasts and myofibroblasts in renal fibrosis. *International J Exp Pathol* 2011;92(3):158-67.

12. Barry-Hamilton V, Spangler R, Marshall D, et al. Allosteric inhibition of lysyl oxidase-like-2 impedes the development of a pathologic microenvironment. *Nat Med* 2010;16(9):1009-17.

13. Schneider DJ, Wu M, Le TT, et al. Cadherin-11 contributes to pulmonary fibrosis: potential role in TGF-beta production and epithelial to mesenchymal transition. *Faseb J* 2012;26(2):503-12.

14. Woroniecka KI, Park AS, Mohtat D, Thomas DB, Pullman JM, Susztak K. Transcriptome analysis of human diabetic kidney disease. *Diabetes* 2011;60(9):2354-69.

15. Cohen CD, Lindenmeyer MT, Eichinger F, et al. Improved elucidation of biological processes linked to diabetic nephropathy by single probe-based microarray data analysis. *PloS One* 2008;3(8):e2937.

16. Lim AK, Ma FY, Nikolic-Paterson DJ, Kitching AR, Thomas MC, Tesch GH. Lymphocytes promote albuminuria, but not renal dysfunction or histological damage in a mouse model of diabetic renal injury. *Diabetologia* 2010;53(8):1772-82.

17. Gandolfo MT, Jang HR, Bagnasco SM, et al. Foxp3+ regulatory T cells participate in repair of ischemic acute kidney injury. *Kidney Int* 2009;76(7):717-29.

18. Wang Y, Wang YP, Zheng G, et al. Ex vivo programmed macrophages ameliorate experimental chronic inflammatory renal disease. *Kidney Int* 2007;72(3):290-9.

19. Li B, Castano AP, Hudson TE, et al. The melanoma-associated transmembrane glycoprotein Gpnmb controls trafficking of cellular debris for degradation and is essential for tissue repair. *Faseb J* 2010;24(12):4767-81.

20. Ramachandran P, Pellicoro A, Vernon MA, et al. Differential Ly-6C expression identifies the recruited macrophage phenotype, which orchestrates the regression of murine liver fibrosis. *Proc Natl Acad Sci USA* 2012;109(46):E3186-95.

21. Lin SL, Li B, Rao S, et al. Macrophage Wnt7b is critical for kidney repair and regeneration. *Proc Natl Acad Sci USA* 2010;107(9):4194-9.

22. Wnuk M, Hlushchuk R, Janot M, et al. Podocyte EphB4 signaling helps recovery from glomerular injury. *Kidney Int* 2012;81(12):1212-25.

23. Hagemann JH, Thomasova D, Mulay SR, Anders HJ. Nrf2 signalling promotes ex vivo tubular epithelial cell survival and regeneration via murine double minute (MDM)-2. *Nephrol Dial Transplant* 2013;28(8):2028-37.

24. Suzuki D, Miyazaki M, Jinde K, et al. In situ hybridization studies of matrix metalloproteinase-3, tissue inhibitor of metalloproteinase-1 and type IV collagen in diabetic nephropathy. *Kidney Int* 1997;52(1):111-9.

25. Parsons CJ, Bradford BU, Pan CQ, et al. Antifibrotic effects of a tissue inhibitor of metalloproteinase-1 antibody on established liver fibrosis in rats. *Hepatology* 2004;40(5):1106-15.

Table 1. Pathological parameters in each cohort. Data are means (±SD) *p<0.05, ***p<0.001 v Controls; #p<0.05 v Injury cohort

	Control (n=6)	Injury (n=10)	Reversal (n=9)
Kidney weight (g)	1.38±0.10	1.64±0.21*	1.53±0.19
Body weight (g)	460±25.5	350±39.5***	424±33.2##
Kidney/body weight (%)	0.30±0.01	0.47±0.06***	0.36±0.03*#
Mean number of glomeruli per tissue section	181±36.0	169±20.5	171±18.7
Mean hilar glomerular cross-sectional area (%age control)	100	98.0±7.4	100.6±10.0
Mean number of WT1+ cells/hilar glomerular cross-section	13.6±1.5	11.5±1.8	11.8±1.7

Table 2. Metacore process networks and Ingenuity Pathways which are over-represented amongst genes that are up-regulated specifically during injury

	p-value
Matacore Process Network	
Cell adhesion: cell-matrix interactions	3.22×10^{-12}
Development: cartilage development	1.14×10^{-7}
Cell adhesion: platelet-endothelium-leucocyte interactions	3.94×10^{-7}
Cell adhesion: integrin-mediated cell-matrix interactions	1.99×10^{-5}
Development: regulation of epithelial-to-mesenchymal transition	2.24×10^{-4}
Cell adhesion: glycoconjugates	6.94×10^{-4}
Ingenuity Pathway Analysis	
Hepatic fibrosis/Hepatic stellate cell activation	9.55×10^{-7}
Complement system	2.19×10^{-6}
Acute phase response signalling	1.74×10^{-5}
Intrinsic prothrombin activation pathway	5.62×10^{-5}
Agranulocyte adhesion and diapedesis	5.50×10^{-4}
Role of pattern recognition receptors in recognition of bacteria and viruses	8.51×10^{-4}
Coagulation system	1.66×10^{-3}
Glioma invasiveness signalling	5.50×10^{-3}
Cell cycle: G2/M DNA damage checkpoint regulation	5.50×10^{-3}
Role of Osteoblasts, osteoclasts and chondrocytes in rheumatoid arthritis	8.13×10^{-3}
14-3-3-mediated signalling	1.17×10^{-2}
Fc epsilon RI signalling	2.00×10^{-2}
PDGF signalling	2.40×10^{-2}
Sertoli cell-Sertoli cell junction signalling	3.24×10^{-2}
3-phosphoinositide degradation	3.63×10^{-2}

Table 3. Metacore process networks and Ingenuity Pathways which are over-represented amongst genes that remain persistently up-regulated during the reversal phase

	p-value
Metacore Process Network	
Immune response: T-cell receptor signalling	1.96×10^{-5}
Signal transduction: Wnt signalling	3.58×10^{-4}
Development: blood vessel morphogenesis	4.18×10^{-4}
Cell adhesion: cell-matrix interactions	6.58×10^{-4}
Apoptosis: apoptosis stimulation by external signals	7.78×10^{-4}
Immune response: antigen presentation	9.88×10^{-4}
Immune response: phagocytosis	1.03×10^{-3}
Cytoskeleton: regulation of cytoskeletal rearrangement	1.63×10^{-3}
Ingenuity Pathway	
LPS/IL-1 mediated inhibition of RXR function	8.32×10^{-3}
Ceramide signalling	1.62×10^{-2}
ERK/MAPK signalling	1.86×10^{-2}
Apoptosis signalling	2.00×10^{-2}
Cardiac β-adrenergic signalling	2.29×10^{-2}
Wnt/β-catenin signalling	2.45×10^{-2}
RhoA signalling	2.69×10^{-2}
Ephrin receptor signalling	2.95×10^{-2}
Protein Kinase A signalling	3.09×10^{-2}
Nrf2-mediated oxidative stress response	3.16×10^{-2}
P70S6K signalling	3.39×10^{-2}
Telomerase signalling	3.55×10^{-2}
Colorectal cancer metastasis signalling	3.80×10^{-2}
Tec kinase signalling	3.98×10^{-2}
Rac signalling	4.57×10^{-2}
3-phosphoinositol biosynthesis	4.79×10^{-2}

Figure legends

Figure 1. Albuminuria progressively increases during 28 weeks of hypertension and hyperglycaemia, but diminishes rapidly following relative normalisation of blood glucose and blood pressure. **A.** Schemata of the study design. **B.** Blood glucose concentration **C.** Blood pressure and **D.** Albumin:Creatinine ratio (ACR) in the injury and reversal cohorts and in controls. Data given are means (±SEM). *p<0.05, **p<0.01 v at peak injury

Figure 2. 28 weeks of hyperglycaemia and hypertension resulted in a significant increase in glomerulosclerosis and tubulointerstitial fibrosis, which was not reversed following eight weeks of relative normalisation of blood sugar and blood pressure. **A.** Representative periodic-acid schiff staining in the glomeruli with quantification of the glomerulosclerosis index. **B.** Representative Picosirius Red staining in the tubulointerstitium with quantification of the tubulointerstitial fibrosis index. Scale bars represent 20μM and 100μM in the glomerular and tubulointerstitial images, respectively. Data given are means (±SEM) **p<0.01 and ***p<0.001 v controls

Figure 3. Patterns of differential gene expression in the injury and reversal cohorts. By comparing the relative gene expression in the renal cortex of the injury and reversal cohort with control rats we identified that: 85 genes were up-regulated specifically during injury and reverted towards control levels in the reversal cohort; 314 genes remained persistently up-regulated despite relative normalisation of blood glucose and blood pressure; 80 genes were persistently repressed during both injury and repair; four genes were down-regulated during injury, but returned towards normal levels following normalisation of blood glucose and blood pressure; 19 and five genes were not differentially expressed during injury, but were down- or up-regulated, respectively, during reversal.

Figure 4A. Relative expression of myofibroblast markers (transgelin, α-smooth muscle actin) and prototypic ECM genes (fibronectin and the α-1 chain of type I collagen). **B.** Number of **i.** total (ED-1^{+}) **ii.** classically activated (inducible nitric oxide (NOS^{+})) and **iii.** mannose receptor+ macrophages in the injury and reversal cohorts and in control animals. **Ci.** Number of CD3^{+} T-cells per x400-power tubulointerstitial field and **ii.** relative expression of the *Foxp3* gene in the injury and reversal cohorts and in controls *p<0.05, **p<0.01 and ***p<0.001 v controls; $^{\#}$p<0.05, $^{\#\#}$p<0.01, $^{\#\#\#}$p<0.001 v injury cohort

Figure 5. Despite increased MMP gene expression, MMP activity was reduced during injury and reversal compared with controls, but this could be restored by physical separation of the MMP:TIMP complexes during zymography. **A.** Relative expression of the Mmp-2, -7, -12 and -14 genes; **B.** Mean gelatinase and collagenase activity and **C.** Relative expression of **i.** TIMP genes and **ii**. TIMP-1 protein by Western blotting with quantification by densitometry in the renal cortex of controls and in the injury and reversal cohorts. **D.** Representative images and quantification of **i.** gelatinase and **ii.** collagenase zymography, demonstrating activity of MMP-2 (72kD band) and MMP-1 (52kD band) respectively. Data given are means (±SEM). *p<0.05, *p<0.01 and ***p<0.001 v controls; $^{\#\#}$p<0.01 and $^{\#\#\#}$p<0.001 v injury cohort

Supplementary Figure. There was a non-significant trend (p=0.07) towards a reduction in the number of WT1+ podocytes in animals from both the injury and reversal cohorts compared to controls. Figure shows representative images of WT1 staining in the glomeruli from animals in each group. Scale bars represent 20μM

Figure 1

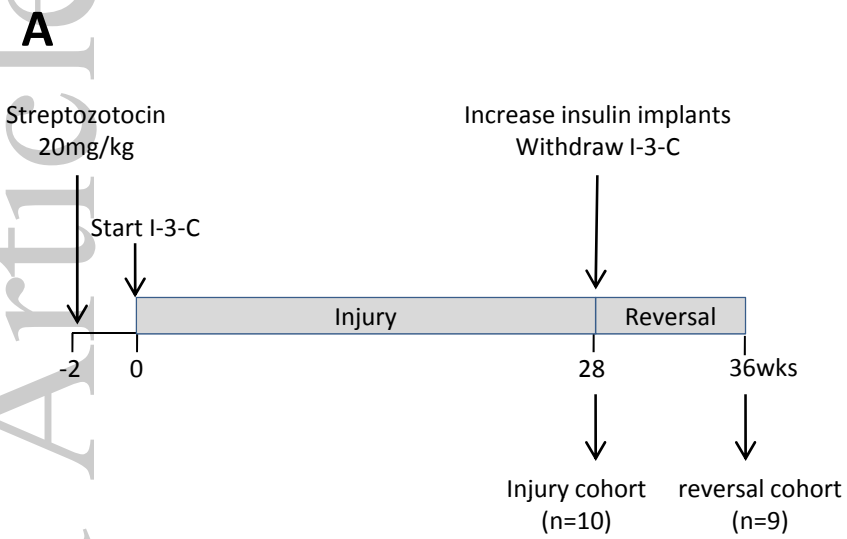

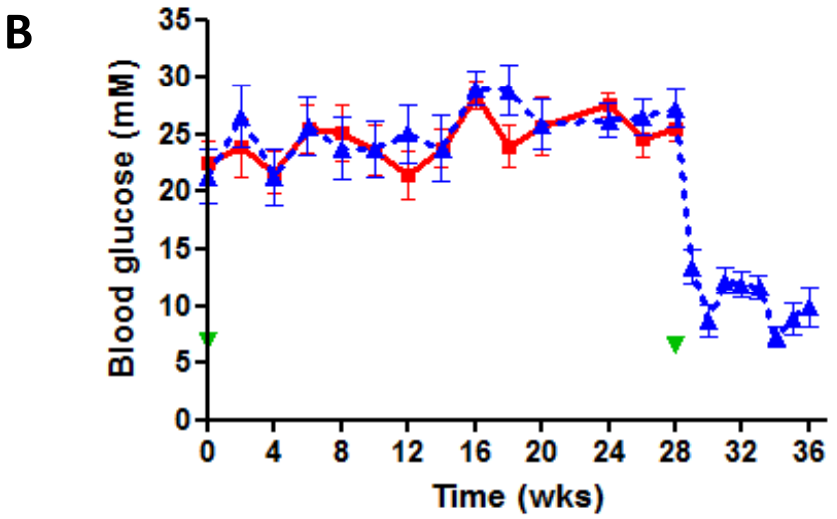

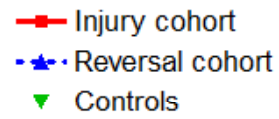

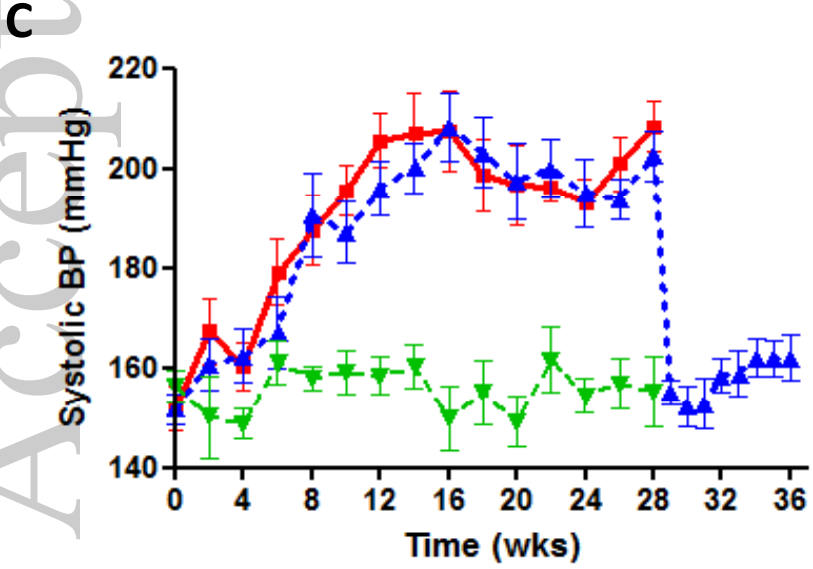

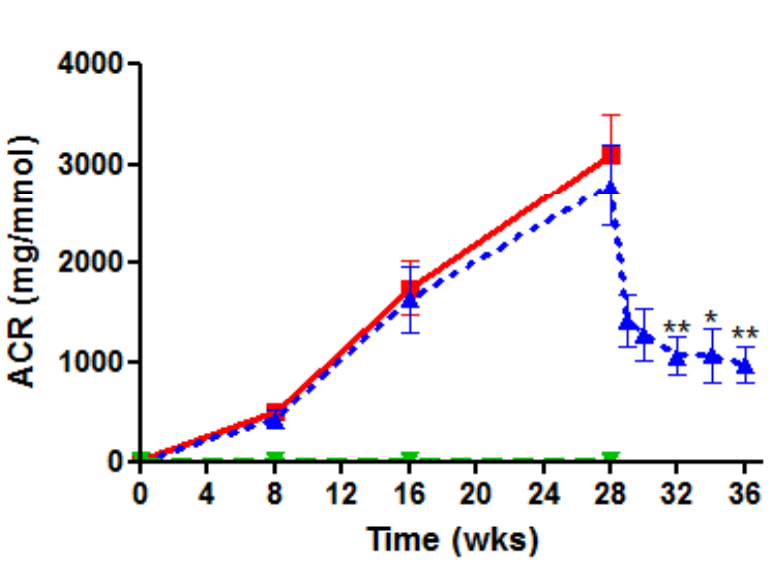

Figure 2A

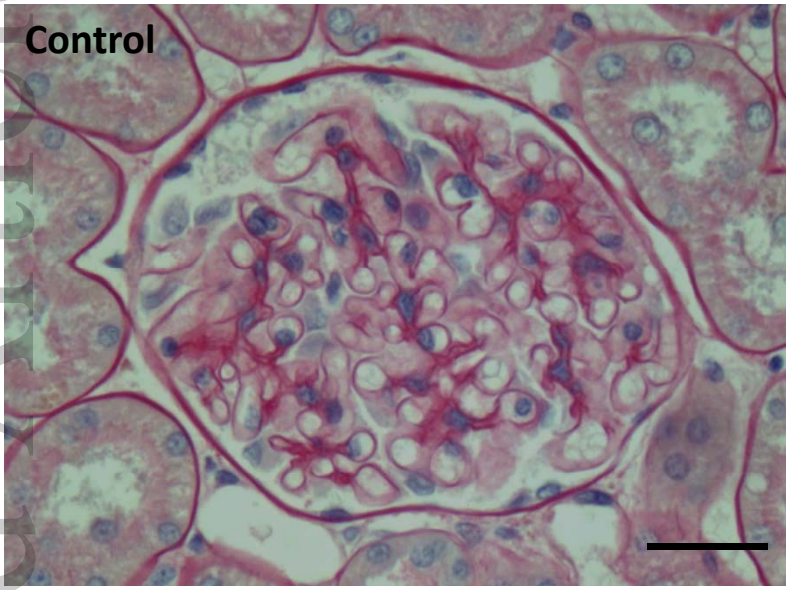

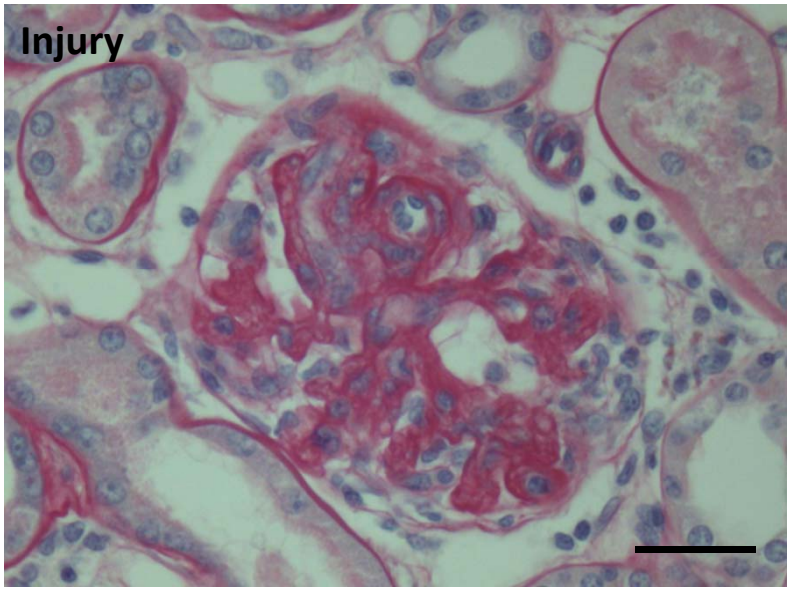

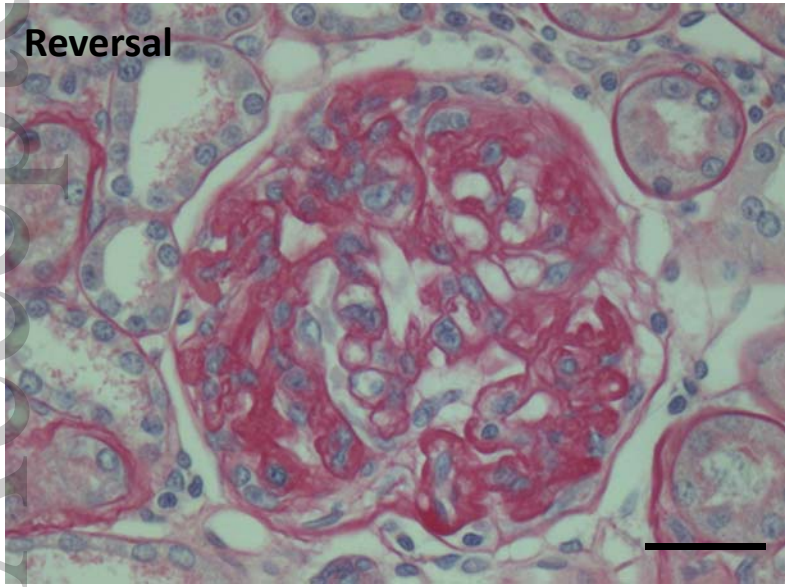

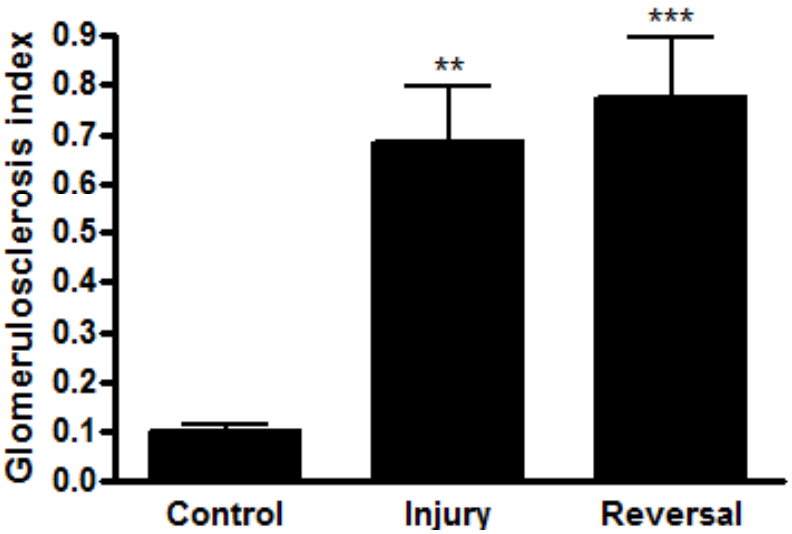

Figure 2B

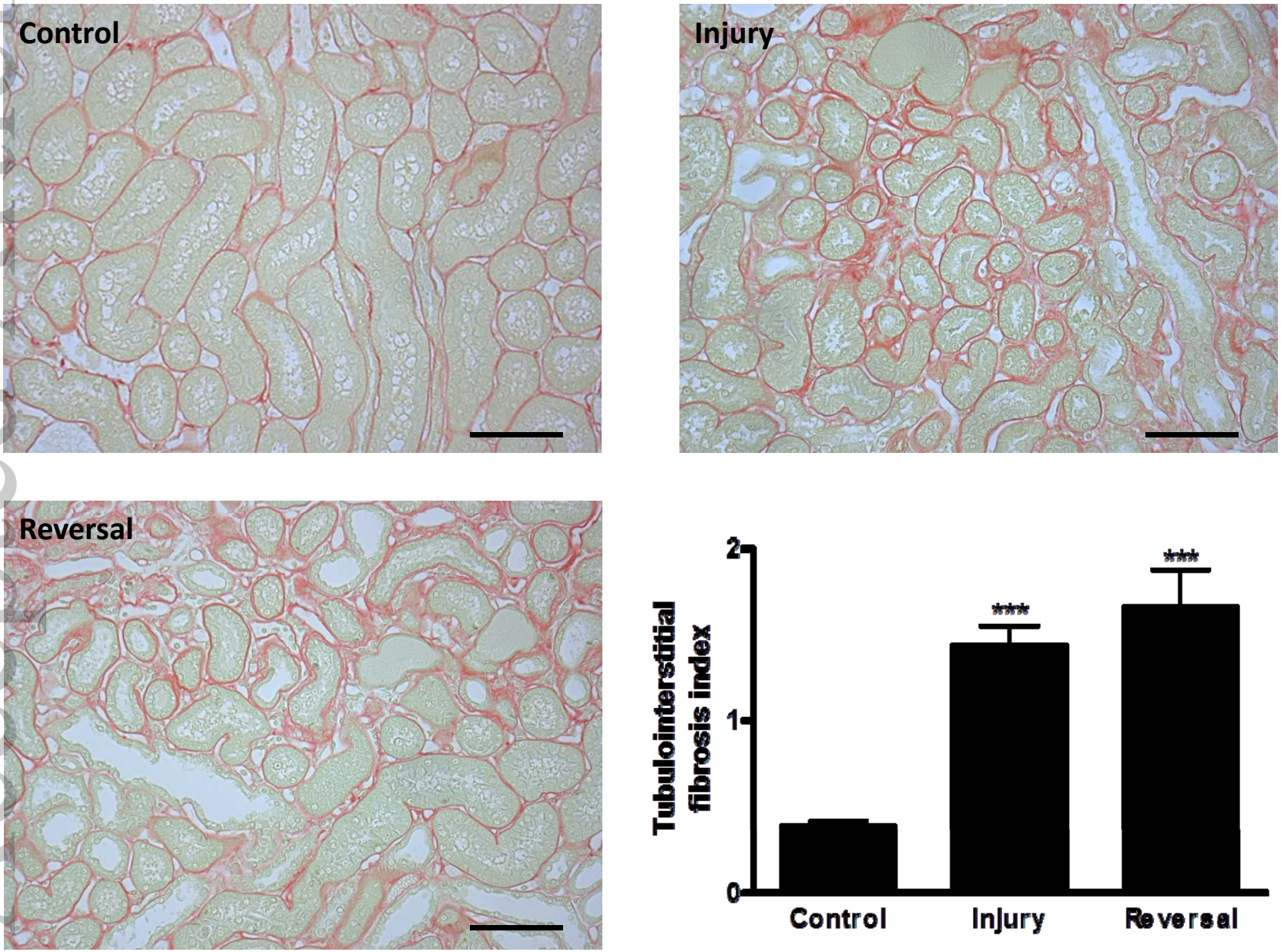

Figure 3

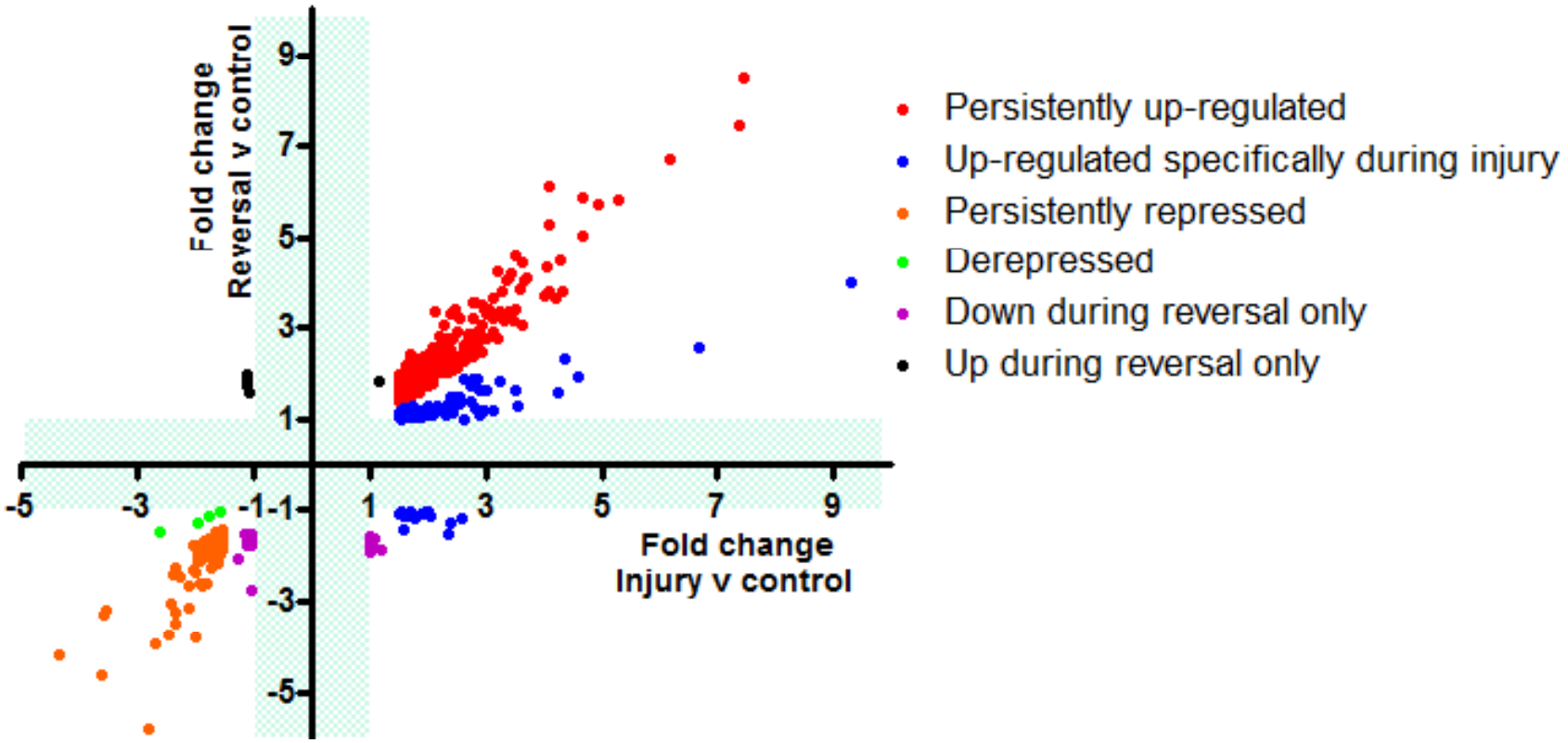

Figure 4A

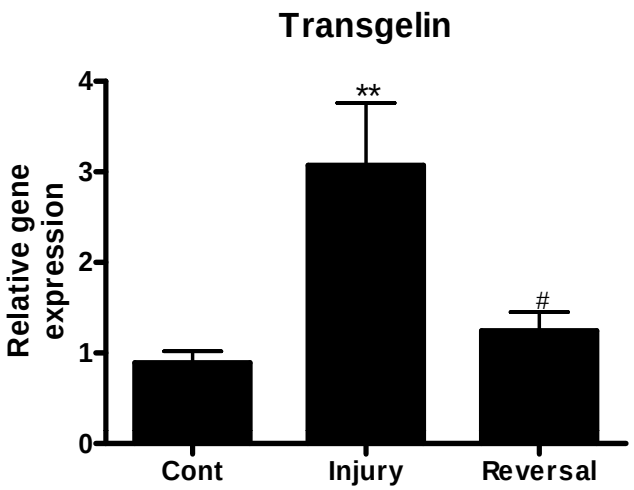

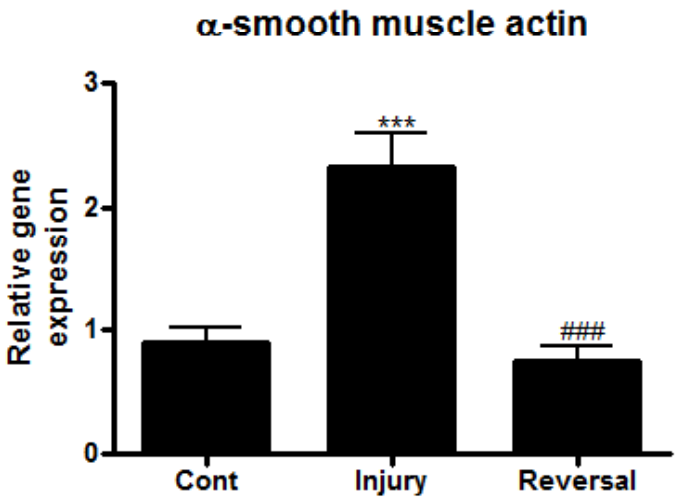

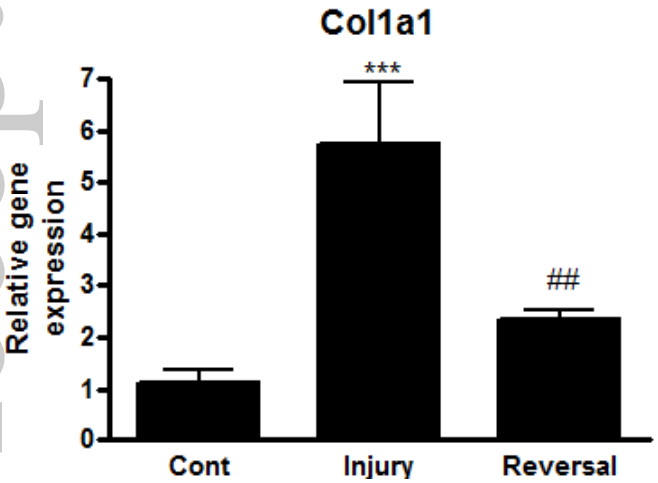

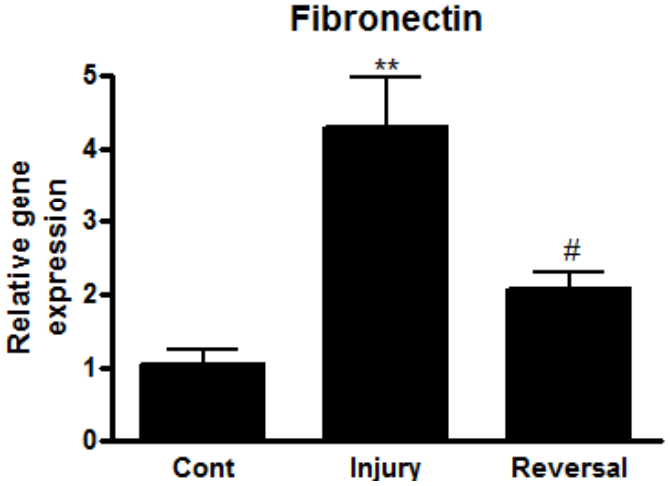

Bi

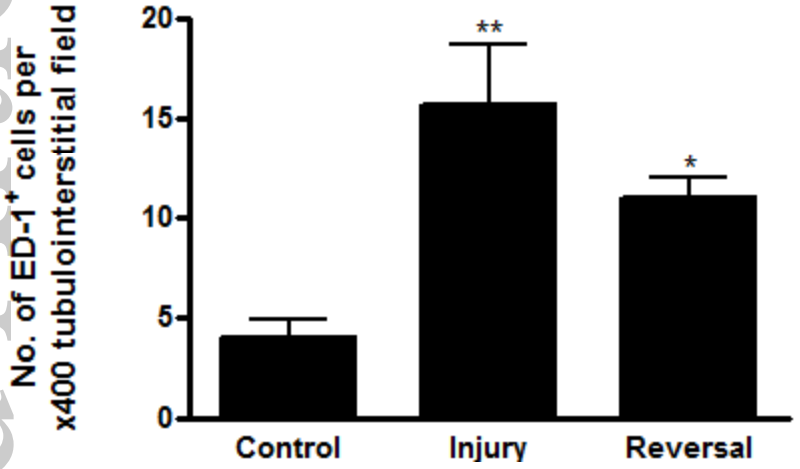

Bii

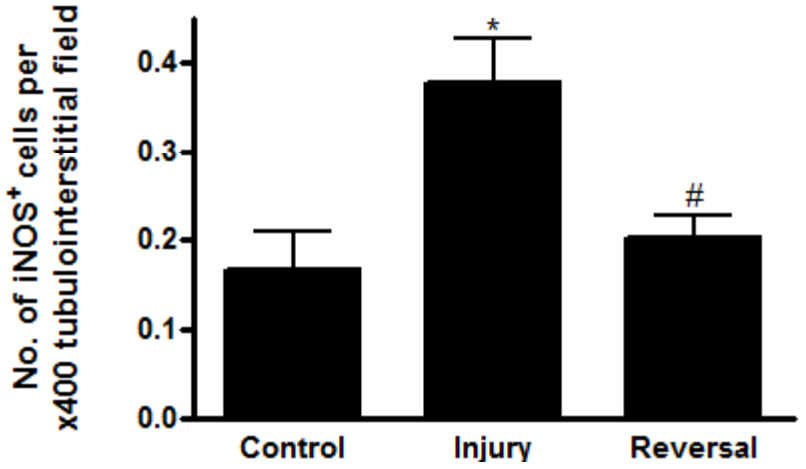

Biii

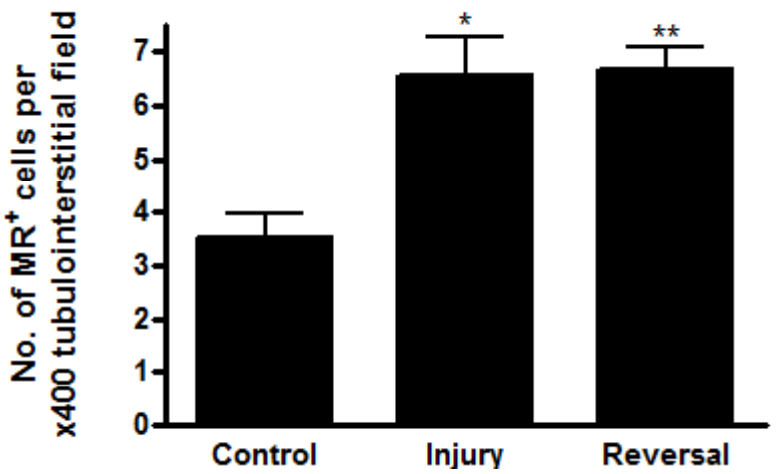

Ci

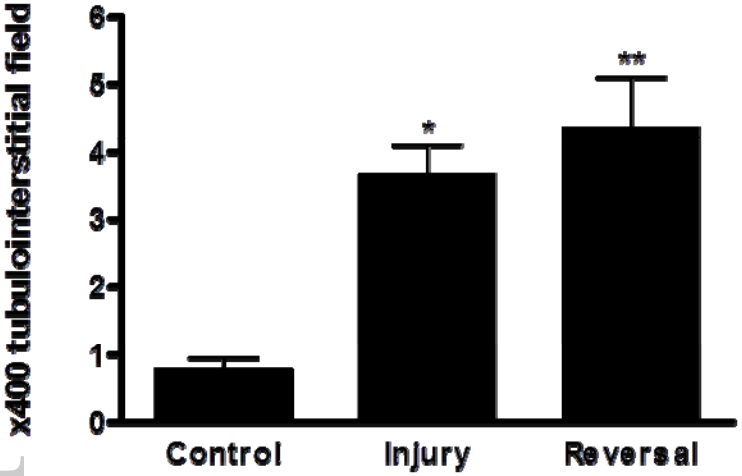

Cii

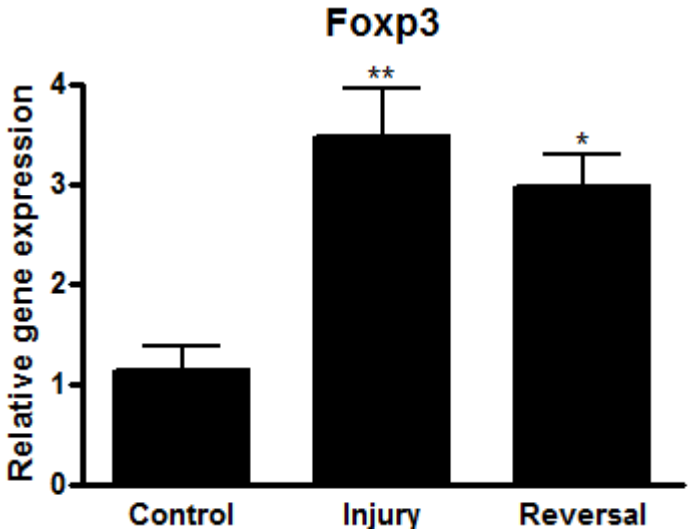

Figure 5A

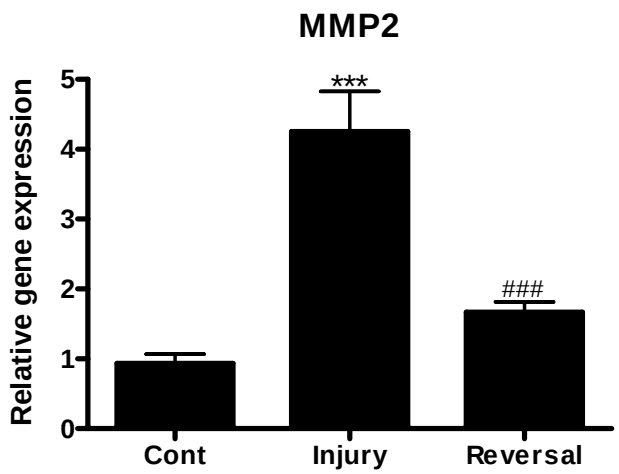

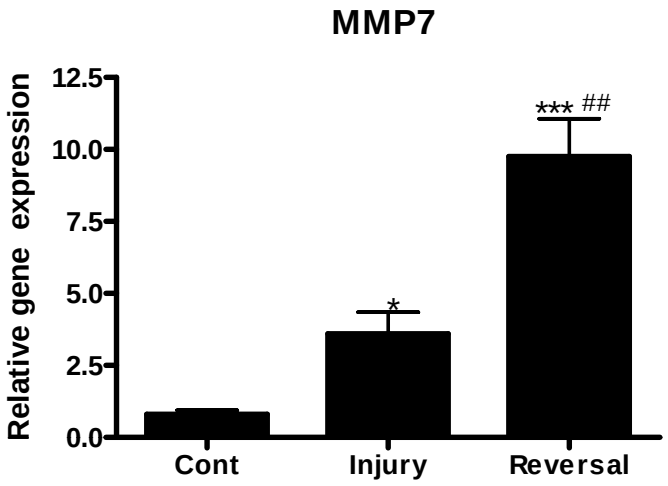

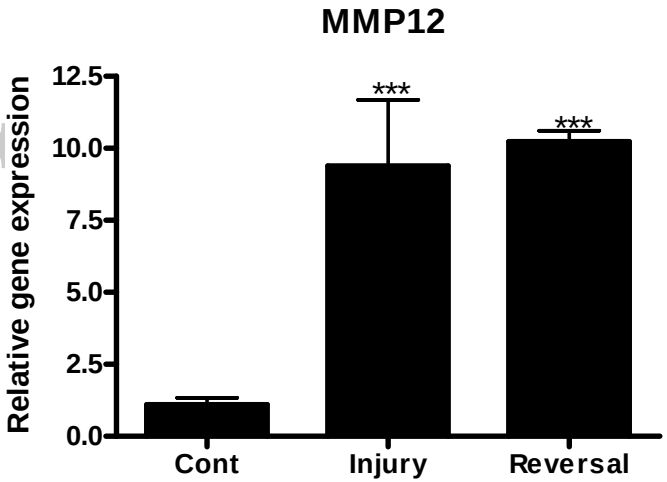

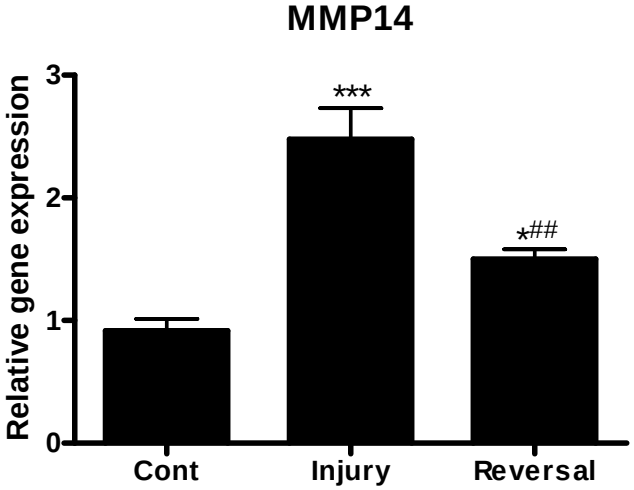

Figure 5B

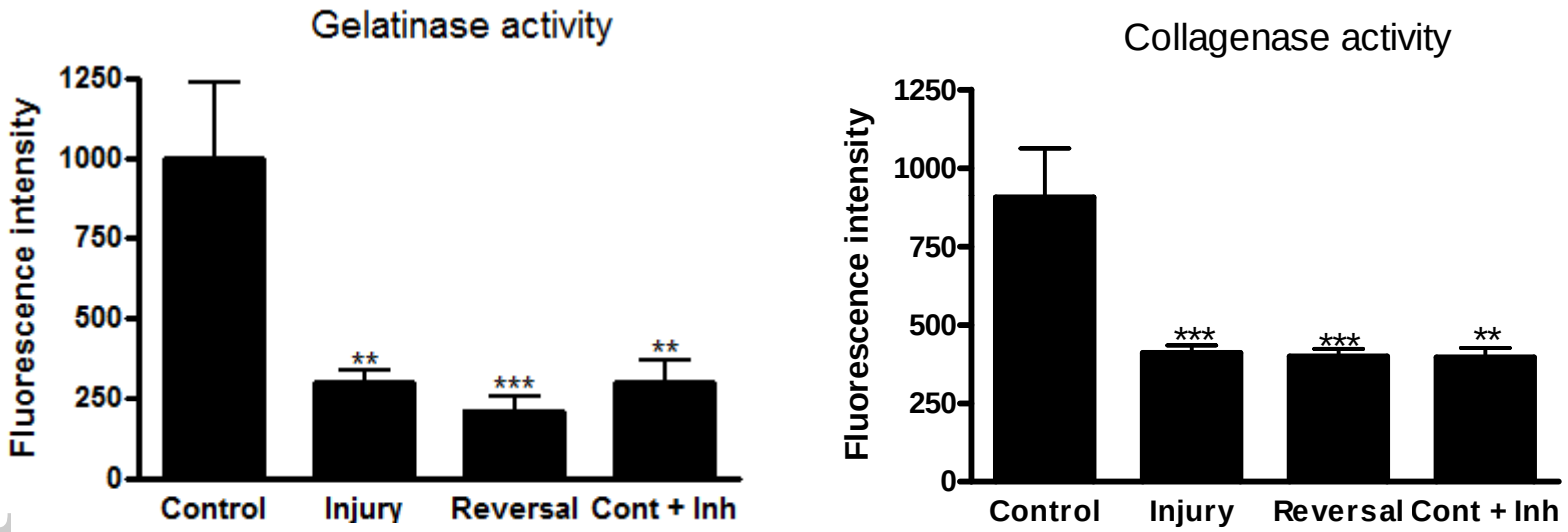

Figure 5C

i

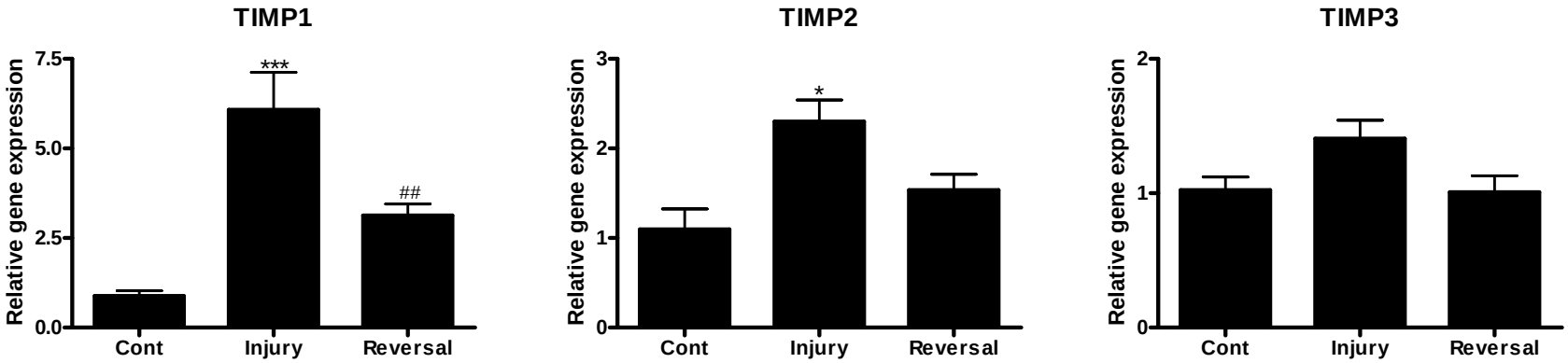

ii

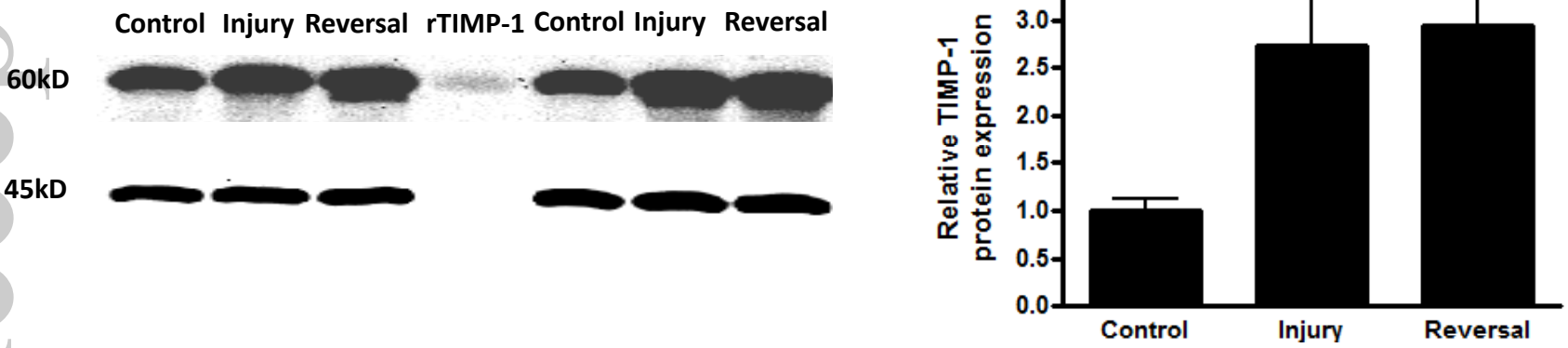

Figure 5D